To be presented at the 2025 European Control Conference, June 2025, Thessaloniki, Greece.

A frequency-domain approach for estimating continuous-time diffusively coupled linear networks

Desen Liang, E.M.M. (Lizan) Kivits, Maarten Schoukens and Paul M.J. Van den Hof

***Abstract*— This paper addresses the problem of consistently estimating a continuous-time (CT) diffusively coupled network (DCN) to identify physical components in a physical network. We develop a three-step frequency-domain identification method for linear CT DCNs that allows to accurately recover all the physical component values of the network while exploiting the particular symmetric structure in a DCN model. This method uses the estimated noise covariance as a non-parametric noise model to minimize variance of the parameter estimates, obviating the need to select a parametric noise model. The method is illustrated with an application from In-Circuit Testing of printed circuit boards. Experimental results highlight the method's ability to consistently estimate component values in a complex network with only a single excitation.**

I. INTRODUCTION

Physical dynamic networks consist of interconnections of physical components, which can be described by diffusive couplings. They can model various processes in numerous fields, such as electrical circuits, mechanical machines, and chemical processes [1]. System identification uses statistical methods to construct mathematical models of dynamical systems from measured data [2] and is widely used in fault detection and diagnosis (FDD) [3]. As physical systems such as printed circuit board assemblies (PCBAs) grow in complexity, there is an increasing interest in physical network identification to effectively identify the dynamics of interconnected systems. One application of this technique is In-Circuit Testing, which diagnoses faults in PCBAs by utilizing data from test probes. As PCBAs can be modeled as physical dynamic networks, the idea is to estimate each electronic component value with the network structure, compare it with the expected value, and analyze the difference in values to verify its correctness.

Several data-driven methods are available to identify physical components in networks. For example, physical systems can be identified by estimating structured state-space models [4] [5]; physical systems can also be treated as directed dynamic networks with specific structural constraints in [6], where prediction error methods are used for estimation. As a more direct approach, a DCN model has been developed in [7] where the physical system is represented as a non-directed network, and a discrete-time (DT) multistep algorithm has been developed to identify structured polynomial models of DCNs incorporating the network structure. The structured polynomials directly represent the physical component values of the network. However, since physical component values are most often represented in the continuous-time domain, there is a need for developing an estimation algorithm for estimating a continuous-time model in the same DCN setting. This will be the topic of the current paper.

Numerous estimation methods involving instrumental variables have been used to identify CT models [8] [9]. Indirect and direct CT identification approaches for dynamic networks that are modeled as interconnected CT transfer functions have been developed in [10]. Frequency domain-based techniques have been applied to identify CT and DT models directly within the same algorithm. Alternatively, CT systems with multiple inputs and multiple outputs (MIMO) can be identified using a two-step frequency-domain approach by first estimating the non-parametric frequency response functions (FRF) and a frequency-dependent noise covariance, and then using these to identify parametric transfer function models [11]–[13]. Utilizing these two-step methods, a local module identification method in dynamic networks has been proposed in [14]. As the physical component values are intertwined within the transfer function's coefficients, it is preferable and straightforward to retrieve these values from the structured polynomial matrix of the DCN model. Therefore, in this paper, we aim to develop a method that directly identifies CT DCNs while preserving the physical network structure, enabling accurate estimation of the network's physical components.

The research question we aim to answer in this paper is: *How can we consistently identify the physical component values in a DCN model in CT?* This paper addresses this problem by directly identifying a CT DCN model in the frequency domain. An identification procedure is developed by extending the frequency-domain approach in [13] to DCNs, and a consistent estimation is shown.

After presenting the DCN and its frequency-domain model in Section II, we present a three-step frequency-domain identification algorithm in Section III. This algorithm will be applied to an In-Circuit testing experiment, of which the results are shown and discussed in Section IV. The conclusion is provided in Section V.

We consider the following notation throughout the paper. $A(p)$ is a polynomial matrix with $A(p) = \sum_{\ell=0}^{n_a} A_\ell p^\ell$, and its (j,k)-th element $[A(p)]_{jk} := a_{jk}(p) = \sum_{\ell=0}^{n_a} a_{jk,\ell} p^\ell$.

Funded by the European Union. Views and opinions expressed are however those of the author(s) only and do not necessarily reflect those of the European Union or the European Research Council. Neither the European Union nor the granting authority can be held responsible for them.

The authors are/were with the Control Systems Group, Department of Electrical Engineering, Eindhoven University of Technology, The Netherlands. d.liang.cn@outlook.com, {m.schoukens, p.m.j.vandenhof}@tue.nl. Lizan Kivits is now with the Dutch Institute for Fundamental Energy Research (DIFFER). e.m.m.kivits@differ.nl.

II. DIFFUSIVELY COUPLED NETWORKS

A. Continuous-time model

A linear diffusive coupling describes an interconnection among node signals in which the coupling strength is proportional to the signal difference between the nodes. This coupling yields symmetric interactions for the linear components. We can describe the full dynamics and topology of linear DCNs as follows according to [7].

Definition 1 *(DCN) A DCN consisting of L node signals, collected in $w(t)$, and K excitation signals $r(t)$, is described as*

$$A(p)w(t) = B(p)r(t) + F(p)e(t), \tag{1}$$

where p is the differential operator, i.e., $p^\ell w_j(t) = w_j^{(\ell)}(t)$, $w_j^{(\ell)}(t)$ is the ℓ-th order derivative of node signals $w_j(t)$,

- *$A(p) = \sum_{\ell=0}^{n_a} A_\ell p^\ell \in \mathbb{R}^{L\times L}[p]$, with $a_{jk}(p) = a_{kj}(p)$, $\forall k, j$, and $A^{-1}(p)$ is stable.*
- *$B(p) \in \mathbb{R}^{L\times K}[p]$.*
- *$F(p) \in \mathbb{R}^{L\times L}(p)$ is monic, stable, rational, and the inverse matrix is also stable.* □

The DCN is assumed to be connected, which means that there is a path between each pair of nodes. The polynomial matrix $A(p)$ is symmetric and non-monic, capturing the symmetric diffusive couplings in the system. The polynomial matrix $B(p)$ characterizes the dynamics through which the excitation signals $r(t)$ enter the network and is chosen in this paper as binary and known. To model the unknown disturbance signals, $F(p)$ is a rational matrix that captures the noise dynamics, and $e(t)$ represents a wide-sense stationary white noise process that is independent and identically distributed (i.i.d.). The input/output signals follow the band-limited measurement assumption.

Remark 1 *Note that pre-multiplying* (1) *with $A^{-1}(p)$ yields a transfer function form. If $F(p)$ is a polynomial or identity matrix, the model* (1) *yields a non-monic ARMAX-like or non-monic ARX-like model structure, respectively. In this paper, $F(p)$ is chosen as a polynomial matrix, resulting in a nonmonic ARMAX-like model structure.* □

We can reformulate (1) by decomposing $A(p)$ into $X(p)+Y(p)$ as

$$X(p)w(t) + Y(p)w(t) = B(p)r(t) + F(p)e(t), \tag{2}$$

where $X(p)$ is a diagonal polynomial matrix which represents the grounded dynamics of the DCN; $Y(p)$ is a Laplacian[1] polynomial matrix of which the off-diagonal elements represents the interconnected dynamics of the DCN. The symmetric polynomial matrix $A(p) = X(p) + Y(p)$ is used to represent the dynamics of the DCN through which $X(p)$ and $Y(p)$ can be uniquely recovered.

[1]A Laplacian matrix is a symmetric matrix with nonpositive off-diagonal elements and with nonnegative diagonal elements that are equal to the negative sum of all other elements in the same row (or column) [15].

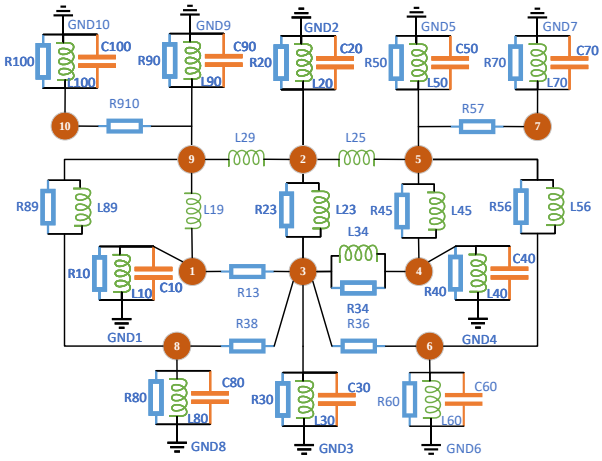

Fig. 1. A 10-node RLC circuit with inductors (L_{jk}), resistors (R_{jk}), capacitors (C_{jk}), and ground nodes(GND_j).

For example, in the 10-node RLC circuit of Fig. 1, $X_{33}(p)$ contains the dynamics of C_{30}, R_{30}, and L_{30}; while $Y_{23}(p) = Y_{32}(p)$ contains the dynamics of R_{23}, and L_{23}.

B. Frequency-domain model

Consider the DCN system described in (1) where CT signals $w(t)$, $r(t)$, and $e(t)$ are sampled in time intervals $t_n = n_s T_s$ ($n_s = 0, ..., N-1$) with a sampling time T_s. The Discrete Fourier Transform (DFT) is used to transform the time-domain model to the frequency-domain. The DFT samples $S(k)$ for the signal $s(t_n)$ are defined as

$$S(k) = \frac{1}{\sqrt{N}} \sum_{t_n=0}^{N-1} s(t_n) e^{-j2\pi k t_n/N}. \tag{3}$$

Applying this DFT to the signals $w(t_n)$, $r(t_n)$, and $e(t_n)$ results in samples $W(k)$, $R(k)$, and $E(k)$, respectively. Accordingly, the DCN frequency-domain model is obtained.

Definition 2 *(Frequency-domain model) The frequency-domain DCN model is defined as*

$$A(\Omega_k)W(k) = B(\Omega_k)R(k) + F(\Omega_k)E(k) + C(\Omega_k). \tag{4}$$

Pre-multiplying with $A^{-1}(\Omega_k)$ on both side gives

$$W(k) = \underbrace{A^{-1}(\Omega_k)B(\Omega_k)}_{G(\Omega_k)} R(k) + \underbrace{A^{-1}(\Omega_k)F(\Omega_k)}_{H(\Omega_k)} E(k) + \underbrace{A^{-1}(\Omega_k)C(\Omega_k)}_{T(\Omega_k)}, \tag{5}$$

where Ω_k is the frequency variable for sample k ($k = 1, ..., N$) and defined as $\Omega_k = j\omega_k$ in CT and $\Omega_k = e^{j\omega_k T_s}$ in DT, $\omega_k = \frac{2\pi k f_s}{N}$ and $f_s = \frac{1}{T_s}$ is the sampling frequency; $G(\Omega_k) \in \mathbb{C}^{L\times K}$ is the input/output dynamics, and $H(\Omega_k) \in \mathbb{C}^{L\times L}$ is the noise model; $T(\Omega_k) \in \mathbb{C}^{L\times 1}$ is the transient term including the system and noise transient in time domain, which cause leakage errors in the frequency domain [11]. □

Moreover, for using the non-parametric noise model later in the paper, the Ω_k-dependent noise covariance is defined as

$$C_V(k) = Cov(V(k)), \text{with } V(k) = H(\Omega_k)E(k). \tag{6}$$

III. FREQUENCY-DOMAIN IDENTIFICATION

In this section a three-step frequency-domain identification approach is presented to consistently estimate the physical components in a DCN. The FRF and frequency-dependent noise covariance are estimated in the first step using a non-parametric methodology. In the second step a parametric DCN model is estimated on the basis of the FRF and a non-parametric noise model, through linear regression steps in a Sanathan-Koerner-type of iteration. In the third step this parametric model is refined through a (nonconvex) maximum likelihood estimation (MLE). This approach offers two main advantages: (1) avoiding the noise model parameterization and the need to determine its structure and order; (2) with the transient term removed in the non-parametric model, the FRF estimation serves to extract "transient-free" input/output data, facilitating the parametric identification.

A. Step 1: non-parametric identification

The first step is to estimate the FRF $G(\Omega_k)$ and the frequency-dependent noise covariance $C_V(k)$. We will use the Local Polynomial Method (LPM) [13], which is an advanced approach to accurately estimate the non-parametric FRF and noise covariance matrix, and that is currently favoured over more classical windowing approaches. It is applicable to general i/o data, i.e. also to non-periodic excitation [13]. In this paper, LPM is implemented using the 'Frequency Domain Toolbox' in [13]. Following the LPM method [13], we estimate polynomials over a short frequency range to obtain a local smooth least-squares approximation of the frequency functions. The FRF $G(\Omega_k)$ and the transient term $T(\Omega_k)$ of the network model (5) are approximated around the selected central frequency k in each frequency band $k+r$ with $r=-n,-n+1,...0,...,n-1,n$,

$$W(k+r)=\left[G\left(\Omega_k\right)+\sum_{s=1}^{\tau}g_s(k)r^s\right]R(k+r) + T\left(\Omega_k\right)+\sum_{s=1}^{\tau}t_s(k)r^s+V(k+r), \quad (7)$$

$$=\Theta Z(k+r)+V(k+r), \quad (8)$$

where τ is the order of the polynomial; $L\times(\tau+1)(K+1)$ matrix Θ collects all the polynomial coefficients as $\Theta = [\ G\left(\Omega_k\right)\quad g_1(k)\quad ...\quad g_\tau(k)\quad T\left(\Omega_k\right)\quad t_1(k)\quad ...\quad t_\tau(k)\ ]$; and $(\tau+1)(K+1)\times 1$ vector Z collects the input data. Collecting (8) in the frequency band $k+r$ ($2n+1$ samples) at central frequency k and stacking them in a matrix gives

$$W_n=\Theta Z_n+V_n, \quad (9)$$

where, W_n, Z_n and V_n are $L\times(2n+1)$, $(\tau+1)(K+1)\times(2n+1)$, and $L\times(2n+1)$ matrices, respectively. The parameter matrix estimate $\hat{\Theta}$ at central frequency k is obtained by minimizing a least squares cost function locally

$$\hat{\Theta}=\arg\min_{\Theta}||W_n-\Theta Z_n||_{\mathrm{F}}^2, \quad (10)$$

where, for any matrix M, $||M||_{\mathrm{F}}$ is the Frobenius norm of matrix M. The optimization (10) is solved by using a numerically stable method (the singular value decomposition). The estimated $L\times K$ matrix $\hat{G}(\Omega_k)$ is extracted from $\hat{\Theta}$

$$\hat{G}\left(\Omega_k\right)=\hat{\Theta}_{[:,1:K]}=W_nZ_n^{\mathrm{H}}(Z_nZ_n^{\mathrm{H}})^{-1}_{[:,1:K]}, \quad (11)$$

where M^{H} is the Hermitian conjugate transpose of a complex matrix M and $\hat{\Theta}_{[:,1:K]}$ represents the first K columns extracted from the matrix $\hat{\Theta}$. Finally, substituting the estimation of the polynomial coefficients into (9), we can get the non-parametric noise estimation,

$$\hat{V}_n=W_n-\hat{\Theta}Z_n=W_n[I_{2n+1}-Z_n^{\mathrm{H}}(Z_nZ_n^{\mathrm{H}})^{-1}Z_n]. \quad (12)$$

With this, the estimated noise covariance $\hat{C}_V(k)$ is obtained from the residual of (10) in line with [11],

$$\hat{C}_V(k)=\frac{\hat{V}_n\hat{V}_n^{\mathrm{H}}}{2n+1-(\tau+1)(K+1)}. \quad (13)$$

By varying the central frequency k over all frequencies, we can find the estimates (11) and (13) for the whole range of frequencies.

Remark 2 *The order τ of the polynomials is chosen as 3 to compromise leakage and interpolation error. The quality of the noise model depends only on the frequency bandwidth $2n+1$ and the order of the local polynomial approximation τ. Using this non-parametric noise model avoids performing a model order selection process as is required for classical PEM-based parametric identification.* □

B. Step 2: structured polynomial matrix identification

In this step a parametric DCN model is estimated on the basis of the frequency domain data obtained in Step 1. The method is shown to lead to consistent results, while exploiting a constrained convex optimization.

We consider a parametric model set,

$$\mathcal{M}=\{(A(p,\theta),B(p,\theta),C(p,\theta)),\theta\in\Psi\subset\mathbb{R}^d\}, \quad (14)$$

with $d\in\mathbb{N}$, where θ includes all unknown parameters of the DCN model $A(p),B(p)$ and $C(p)$. Besides, the data generating system $\mathcal{S}$ is denoted by,

$$\mathcal{S}=(A^0(p,\theta^0),B^0(p,\theta^0),C^0(p,\theta^0),F^0(p,\theta^0)). \quad (15)$$

The condition that the data generating system belongs to the considered model set is needed for a consistent estimate. Since the noise model is not parameterized, the noise model is independent of the plant model. We only need $P_0\in\mathcal{M}$ for a consistent estimate in this paper, with $P_0=\left(A^0(p,\theta^0),B^0(p,\theta^0),C^0(p,\theta^0)\right)$.

Proposition 1 *The DCN is identifiable if the following conditions are satisfied according to [7] and [16]:*

1) *The polynomials $A(p)$ and $B(p)$ are left-coprime.*
2) *There exists a permutation matrix P that leads to $[A_0\ A_1\ ...\ A_{n_a}\ B_0\ B_1\ ...\ B_{n_b}]\,P=[D\ U]$ with D square, diagonal, and full rank.*
3) *There is at least one excitation signal, i.e., $K\geq 1$.*

4) *There exists at least one constraint on the parameters of $A(p,\theta)$ and $B(p,\theta)$ that ensures $\Gamma\theta = \upsilon \neq 0$, where Γ is a matrix with full row-rank.* □

Remark 3 *The first condition ensures that there are no common factors between $A(p,\theta)$ and $B(p,\theta)$. The non-monicity of the polynomial matrix $A(p,\theta)$ is addressed in the second and fourth conditions, guaranteeing the uniqueness of this model representation.* □

As the transfer function $G(\Omega_k,\theta)$ is defined as the ratio of two polynomial matrices in (5), a commonly used method to identify this parametric $G(\Omega_k,\theta)$ would be a Gaussian-Newton (GN) based method in which the following nonlinear output error criterion is minimized,

$$\hat{\theta} = \underset{\theta}{\operatorname{argmin}} \frac{1}{N}\sum_{k=1}^{N} ||W(k) - G(\Omega_k,\theta)R(k) - T(\Omega_k,\theta)||_{\mathrm{F}}^2. \tag{16}$$

However, there is no guarantee of reaching the global minimum in such non-convex optimization, possibly leading to inaccurate physical component estimates in the network. To address this problem, we follow the idea of the SK-iteration algorithm [17], where in the i-th step, the parameter estimate is determined by

$$\hat{\theta}^{(i)} = \arg\min_{\theta} \frac{1}{N}\sum_{k=1}^{N} \|A(\Omega_k,\hat{\theta}^{(i-1)})^{-1}\cdot [A(\Omega_k,\theta)W(k) - B(\Omega_k,\theta)R(k) - C(\Omega_k,\theta)]\|_{\mathrm{F}}^2. \tag{17}$$

When the algorithm converges, its stationary point is expected to be close to the global minimum of (16).

In order to arrive at an estimate with reduced variance, it would be attractive to apply an additional frequency weighting to the criteria (16) and (17), reflecting the dynamics of the noise model. The most obvious option for this would be the non-parametric noise model estimate $\hat{C}_V(k)^{\frac{1}{2}}$. However, as shown in [13, Chapter 12] this will also introduce a bias in the estimates, because of the fact that $\hat{C}_V(k)$ and $W(k)$ are not independently distributed.

As an alternative, it is suggested and analyzed in [13, Chapter 12] to employ the sample mean and sample covariance of the node signals $W(k)$, derived from the LPM estimate, as they are asymptotically independently distributed. Utilizing the non-parametric estimate matrix $\hat{\Theta}$ in (10), the sample mean $\hat{W}(k)$ of $W(k)$ is calculated as

$$\hat{W}(k) = \hat{G}(\Omega_k)R(k) + \hat{T}(\Omega_k), \tag{18}$$

where $\hat{G}(\Omega_k)$ is the FRF estimate obtained from $\hat{\Theta}$ in the non-parametric identification part (11) and $\hat{T}(\Omega_k)$ is the transient term given as $\hat{T}(\Omega_k) = \hat{\Theta}_{[:,K(R+1)+1]}$ (the $K(R+1)+1$-th column of $\hat{\Theta}$). The sample covariance $\hat{C}_W(k)$ of $\hat{W}(k)$ can be calculated from the noise covariance model obtained from the non-parametric part as

$$\hat{C}_W(k) = (Z_n^{\mathrm{H}}(Z_n Z_n^{\mathrm{H}})^{-1}Z_n)_{[n+1,n+1]}\hat{C}_V(k). \tag{19}$$

Remark 4 *The asymptotic behaviors and the related proof of the sample mean and sample covariance are shown in [12] and [13, Chapter 12].* □

By replacing $W(k)$ in (17) and the frequency weighting $\hat{C}_V(k)$ with $\hat{W}(k)$ and $\hat{C}_W(k)$, respectively, we can formulate the frequency-domain identification criterion as

$$\hat{\theta}^{(i)} = \arg\min_{\theta} \frac{1}{N}\sum_{k=1}^{N} \left||M_1^{(i-1)}(k,\theta)|\right|_{\mathrm{F}}^2, \tag{20}$$

with

$$M_1^{(i-1)} = \left[\hat{C}_W(k)^{\frac{1}{2}}A(\Omega_k,\theta^{(i-1)})\right]^{-1}\cdot \left[A(\Omega_k,\theta)\hat{W}(k) - B(\Omega_k,\theta)R(k) - C(\Omega_k,\theta)\right]. \tag{21}$$

Collecting all input/output data for all frequencies and the frequency weighting in the regression matrix Q, and the unknown parameters in the vector θ for each iteration,

$$M_1 = Q\theta. \tag{22}$$

Due to the non-monicity of the polynomial matrix $A(p)$ and since the parameters of $A(p)$ and $B(p)$ might be partially known, the resulting estimation is not a standard (weighted) linear regression problem. Constraints have to be take into account to warrant identifiability. Consequently, a constrained iterative weighted least squares (IWLS) optimization using SK-iteration is executed, where the constraints include the known parameters and the interconnection structure. The solution for each iteration of (20) is then given by

$$\hat{\theta} = \arg\min_{\theta} \theta^{\mathrm{H}}Q^{\mathrm{H}}Q\theta, \quad \text{subject to } \Gamma\theta = \upsilon, \tag{23}$$

where the constraint follows Condition 4 in Proposition 1.

Remark 5 *The structure of the regression matrix Q, the unknown parameter vector θ, selection matrix Γ and the constant vector υ are described in [18].* □

The Lagrangian multiplier λ and Karush–Kuhn–Tucker (KKT) conditions can be used to solve this optimization problem, which in each iteration comes down to solving

$$\begin{bmatrix}\hat{\theta}\\ \hat{\lambda}\end{bmatrix} = \begin{bmatrix}2Q^{\mathrm{H}}Q & \Gamma^T\\ \Gamma & \mathrm{O}\end{bmatrix}^{-1}\begin{bmatrix}\mathrm{O}\\ \upsilon\end{bmatrix}, \tag{24}$$

where O is a zero-matrix with proper dimensions, and $\hat{\lambda}$ are the estimated Lagrange multipliers.

C. Step 3: Maximum likelihood estimation

Upon convergence of the SK-iteration in Step 2, a structured polynomial DCN model is obtained, for which consistency and miniumm variance are not guaranteed. Therefore the resulting model of Step 2, is used as an initial estimate for a sample maximum likelihood estimator (SMLE) that is asymptotically unbiased and asymptotically efficient [13], and in this case is given by the non-convex optimization problem

$$\hat{\theta} = \arg\min_{\theta} \frac{1}{N}\sum_{k=1}^{N} ||M_2(k,\theta)||_{\mathrm{F}}^2, \tag{25}$$

with

$$M_2 = \hat{C}_W(k)^{-\frac{1}{2}}\left[\hat{W}(k) - G(\Omega_k,\theta)R(k) - T(\Omega_k,\theta)\right], \tag{26}$$

$$G(\Omega_k,\theta) = A(\Omega_k,\theta)^{-1}B(\Omega_k,\theta), \tag{27}$$

$$T(\Omega_k, \theta) = A(\Omega_k, \theta)^{-1} C(\Omega_k, \theta), \tag{28}$$

where $\hat{W}(k)$ and $\hat{C}_W(k)$ are obtained in (18) and (19), respectively. Since we focus on the values of the components in the physical network, keeping the network structure during the SMLE is essential. The symmetric structure of $A(p)$ is incorporated in the parameterization and the known dynamic $B(p)$ is fixed. The SMLE cost is minimized using the solver 'lsqnonlin' in Matlab.

D. Full network identification algorithm

The steps given above describe the frequency-domain identification procedure, which can be summarized in the following algorithm.

Algorithm 1 *The frequency-domain identification algorithm for diffusively coupled linear networks is given as:*

1) *Apply the LPM method to estimate the non-parametric* $\hat{G}$ *with* (10) *and the noise covariance* $\hat{C}_V$ *with* (13).
2) *Apply the input/output data criterion* (20) *with sample mean* (18) *and covariance* (19) *leading to the IWLS with constraint* (23) *to estimate the parameters* $\hat{\theta}$ *in a structured polynomial model, which is solved by the SK-iteration.*
3) *Use the result* (24) *as an initial estimate for the SMLE* (25) *to obtain asymptotically unbiased and efficient parameter estimates by an iterative non-convex constrained optimization algorithm.* □

Remark 6 *Achieving consistent estimates of DCNs using this algorithm requires satisfying all conditions specified in Proposition 1 for network identifiability. It is also necessary that the true model is one of the candidate parametric models in the model set (*$P_0 \in \mathcal{M}$*), and the system must be excited at sufficient frequencies for data informativity [16].* □

IV. SIMULATION EXPERIMENTS

The following simulation examples serve to illustrate that the component values of a full DCN can be consistently estimated from only a single excitation signal with full nodes measurement using Algorithm 1, in an In-Circuit Testing application. Consider the 10-node RLC circuit as shown in Fig. 1, where each j-th node, $j = 1, \ldots, 10$, has the following measurement components connected to the ground node: $C_{j0} = 2$ μF, $R_{j0} = 500$ Ω, and $L_{j0} = 18$ mH. The coefficients of the components in the interconnections between the nodes are given as θ_{hcomp} in Table II.

This 10-node RLC circuit can be expressed as a second-order CT DCN model (details are shown in [18]). The excitation signal of this model is chosen as the current and the measured node signals are voltages, to maintain the same structure as (1). The orders of the parametric model are $n_a = 2$, $n_b = 1$, and $n_c = 1$. Here, the symmetric $A(p)$ parameters are given as $a_{jj,0} = \frac{1}{L_{j0}}$, $a_{jj,1} = \frac{1}{R_{j0}}$, and $a_{jj,2} = C_{j0}$; and $a_{jk,0} = -\frac{1}{L_{jk}}$, $a_{jk,1} = -\frac{1}{R_{jk}}$, and $a_{jk,2} = -C_{jk}$ for $j \neq k$. The rest of the parameters in $A(p)$ are given as 0 for the absent connections. The parameters of $B(p)$ are given as $b_{jk,1} = 1$ for the k-th excitation entering the j-th node, and the rest of the parameters in $B(p)$ are 0.

TABLE I
EXPERIMENT NUMBERS WITH CORRESPONDING DATA LENGTHS N.

#	1	2	3	4	5
N	10^3	2×10^3	4×10^3	8×10^3	16×10^3
#	6	7	8	9	10
N	32×10^3	64×10^3	128×10^3	256×10^3	512×10^3

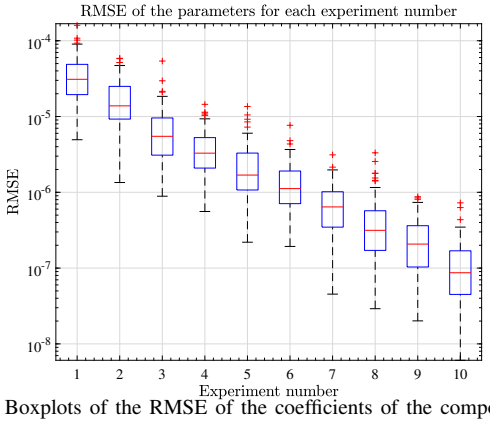

Fig. 2. Boxplots of the RMSE of the coefficients of the components for each experiment.

A. Consistent parameter estimation

The excitation signal $r(t)$ is an independent zero-mean white noise with variance $\sigma_r^2 = 1$ entering only at node 3. The noise signal $e(t)$ is a normal distributed zero-mean white noise with variance $\sigma_e^2 = 1$ entering all nodes. The sampling frequency is set at 20 kHz to cover all the dynamics of the components, and the identification frequency band is set between $f_{min} = 500$ Hz and $f_{max} = 4$ kHz. The constraints incorporate the known input matrix $B(p)$ and the known topology information indicated in the matrix $A(p)$.

To show that the parameters can be consistently estimated with a single excitation, we generated a set of experiments with different data lengths N. The experiment numbers and corresponding values of N are shown in Table I. Each experiment includes 100 Monte Carlo (MC) runs with independent excitation and noise signals.

The box plots of the relative mean squared error (RMSE) of the coefficients of the components for each experiment number are shown in Fig. 2. The relative mean squared error of the coefficients of the components is given as

$$\text{RMSE} = \frac{\|\hat{\theta}_{comp} - \theta^0_{comp}\|_2^2}{\|\theta^0_{comp}\|_2^2}, \tag{29}$$

where $\hat{\theta}_{comp}$ and θ^0_{comp} collect the estimated and actual component values, respectively. The $\hat{\theta}_{comp}$ is uniquely recovered from the estimation of the DCN parameters $\hat{\theta}$. In Fig. 2, it can be seen that the RMSE decreases as N increases, which supports the claim of consistent identification. When the data length N tends to infinity, the estimated parameters converge to the actual parameters.

B. Fault detection and diagnosis

The algorithm for estimating the DCN component values, can be used to detect and diagnose the occurence of faults in any (combination) of the different components in the network. In this Section we will show an example where multiple dynamic faults and open circuits occur simultaneously

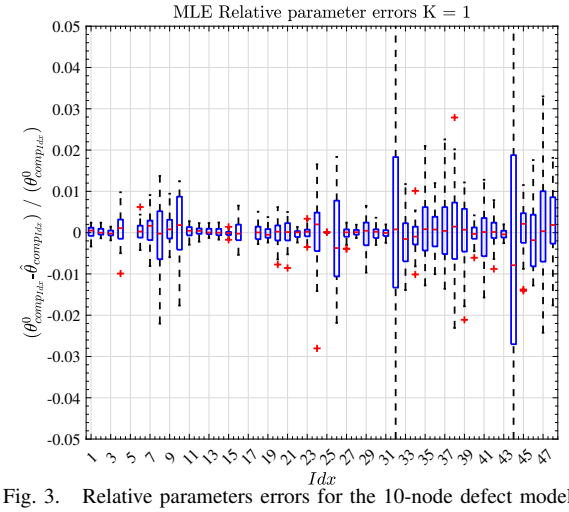

Fig. 3. Relative parameters errors for the 10-node defect model.

in the 10-node RLC network. We consider faulty dynamics in R_{13}, R_{36}, R_{89}, and L_{25} and open circuits in R_{45} and L_{56}, leading to new actual values indicated by θ^0_{comp} in Table II, where the faulty components are indicated in red. We keep the same excitation situation as before and increase the noise power to $\sigma_e^2 = 100$ at all nodes. The data length is $N = 20000$.

The relative parameter errors (RPEs) of the estimation results are shown in Fig. 3. For each ungrounded component, the actual coefficient value (θ^0_{comp}) and the mean estimated coefficient value for 50 MC (CT est) are shown in Table II. It can be seen that all mean estimated values, including the ones for the faulty components, are very close to the actual values. Moreover, all RPEs stay between $\pm 5\%$ for the healthy components as well as for the faulty components (R_{13}, R_{36}, R_{45}, R_{89}, L_{25}, and L_{56}), as shown in Fig. 3. Notice that components Idx 19 to 48, which are the grounded components (arranged in order of C_{j0}, R_{j0}, L_{j0}, $j = 1, \ldots, 10$) show a higher variance compared to the others. This occurs as the interconnected components are represented twice in the model, resulting in the use of more data to estimate these components than is used for the grounded components. This experiment shows that all components are identified correctly. By comparing the identified results with the ideal healthy components, we can detect the physical value changes of the components and diagnose the faults. This shows that the algorithm can be applied to FDD in complex physical networks.

V. CONCLUSIONS

We have introduced a frequency-domain identification method for estimating continuous-time models of diffusively coupled networks. A three-step frequency-domain identification method has been developed that preserves the physical network structure and is used to estimate the values of all physical components in the network. The primary advantages of this method include the direct identification of continuous-time networks and the accurate recovery of the values of physical components in the networks. A successful application to fault detection and diagnosis in In-Circuit Testing in a PCBA has been shown.

TABLE II

10-NODE DEFECT NETWORK COMPONENT VALUES.

Idx	Comp	θ_{hcomp}	θ^0_{comp}	CT est	Unit
1	R_{13}	100	200	200.06	Ω
2	R_{23}	200	200	200.04	Ω
3	R_{34}	150	150	149.98	Ω
4	R_{36}	180	500	500.40	Ω
5	R_{45}	350	Inf	Inf	Ω
6	R_{38}	180	180	180.37	Ω
7	R_{56}	160	160	160.15	Ω
8	R_{57}	120	120	119.93	Ω
9	R_{89}	160	500	500.49	Ω
10	R_{910}	120	120	120.13	Ω
11	L_{19}	5	5	5.00	mH
12	L_{29}	3	3	3.00	mH
13	L_{23}	10	10	10.00	mH
14	L_{25}	15	1	1.00	mH
15	L_{34}	12	12	12.00	mH
16	L_{45}	20	20	20.00	mH
17	L_{56}	13	Inf	Inf	mH
18	L_{89}	13	13	13.00	mH

REFERENCES

[1] F. Dörfler, J. W. Simpson-Porco, and F. Bullo, "Electrical networks and algebraic graph theory: Models, properties, and applications," *Proceedings of the IEEE*, vol. 106, no. 5, pp. 977–1005, 2018.

[2] T. Söderström and P. Stoica, *System identification*. Prentice-Hall International, 1989.

[3] D. Miljković, "Fault detection methods: A literature survey," in *2011 Proc. 34th Intern. Convention MIPRO*, pp. 750–755, 2011.

[4] G. Mercère, O. Prot, and J. A. Ramos, "Identification of parameterized gray-box state-space systems: From a black-box linear time-invariant representation to a structured one," *IEEE Transactions on Automatic Control*, vol. 59, no. 11, pp. 2873–2885, 2014.

[5] C. Yu, L. Ljung, and M. Verhaegen, "Identification of structured state-space models," *Automatica*, vol. 90, pp. 54–61, 2018.

[6] E. M. M. Kivits and P. M. J. Van den Hof, "A dynamic network approach to identification of physical systems," in *2019 IEEE 58th Conference on Decision and Control (CDC)*, pp. 4533–4538, 2019.

[7] E. M. M. Kivits and P. M. J. Van den Hof, "Identification of diffusively coupled linear networks through structured polynomial models," *IEEE Trans. Automatic Control*, vol. 68, no. 6, pp. 3513–3528, 2023.

[8] H. Garnier, M. Gilson, H. Muller, and F. Chen, "A new graphical user interface for the CONTSID toolbox for matlab," *IFAC-PapersOnLine*, vol. 54, no. 7, pp. 397–402, 2021.

[9] R. A. González, C. R. Rojas, S. Pan, and J. S. Welsh, "On the relation between discrete and continuous-time refined instrumental variable methods," *IEEE Control Systems Letters*, vol. 7, pp. 2233–2238, 2023.

[10] A. G. Dankers, P. M. J. Van den Hof, and X. Bombois, "Direct and indirect continuous-time identification in dynamic networks," in *53rd IEEE Conf. Decision and Control (CDC)*, pp. 3334–3339, 2014.

[11] R. Pintelon, J. Schoukens, G. Vandersteen, and K. Barbé, "Estimation of nonparametric noise and frf models for multivariable systems—part i: Theory," *Mechanical Systems and Signal Processing*, vol. 24, no. 3, pp. 573–595, 2010.

[12] R. Pintelon, J. Schoukens, G. Vandersteen, and K. Barbé, "Estimation of nonparametric noise and frf models for multivariable systems—part ii: Extensions, applications," *Mechanical Systems and Signal Processing*, vol. 24, no. 3, pp. 596–616, 2010.

[13] R. Pintelon and J. Schoukens, *System identification: a frequency domain approach*. John Wiley & Sons, 2012.

[14] K. R. Ramaswamy, P. Z. Csurcsia, J. Schoukens, and P. M. J. Van den Hof, "A frequency domain approach for local module identification in dynamic networks," *Automatica*, vol. 142, p. 110370, 2022.

[15] M. Mesbahi and M. Egerstedt, *Graph theoretic methods in multiagent networks*. Princeton University Press, 2010.

[16] E. M. M. Kivits and P. M. J. Van den Hof, "Identifiability of diffusively coupled linear networks with partial instrumentation," *IFAC-PapersOnLine*, vol. 52, no. 2, p. 2395–2400, 2023.

[17] C. Sanathanan and J. Koerner, "Transfer function synthesis as a ratio of two complex polynomials," *IEEE Transactions on Automatic Control*, vol. 8, no. 1, pp. 56–58, 1963.

[18] D. Liang, E. M. M. Kivits, M. Schoukens, and P. M. J. Van den Hof, "A frequency-domain approach for estimating continuous-time diffusively coupled linear networks," tech. rep., 2024. ArXiv:2410.18773 [eess.sY].